CERN-TH.6297/91
CPT-91/PE.2608

Bounds on a light scalar in two-Higgs-doublet models

A. Pich[a] , J. Prades[b] and P. Yepes[a]

[a] CERN, CH-1211 Geneva 23, Switzerland
[b] Centre de Physique Théorique, Section 2, C.N.R.S. - Luminy, Case 907
F-13288 Marseille Cedex 9, France

Abstract

LEP data and limits on η', η and π decays are used to set stringent limits on a possible light scalar Higgs in the framework of general two-Higgs-doublet models.

CERN-TH.6297/91
CPT-91/PE.2608
September 1991

1 Introduction

Within the Standard Model (SM), the possibility of a light Higgs boson is already excluded; the present bound being $m_{h^0} > 57$ GeV (95% C.L.) [1]. However, an extended scalar sector with additional degrees of freedom could easily avoid the present experimental limits, leaving the question of a light Higgs open to any speculation. Given the poor understanding of the scalar sector, there is no compelling reason (aside of simplicity) to assume the existence of only one Higgs doublet. Therefore, it is important to explore the phenomenological implications of more complicated Higgs structures.

Models with several scalar doublets are the preferred candidates for a non-minimal scalar sector, since they satisfy $\rho = M_W^2/M_Z^2 \cos^2\theta_W = 1$ at tree level. In fact, two scalar doublets are already present in the minimal supersymmetric extension of the SM [2]. Models of this kind were also discussed a long time ago in the context of the strong CP problem [3] or to generate spontaneous CP violation [4].

In this paper we investigate the present experimental constraints on a very light neutral scalar ($m_{h^0} < 2\,m_\mu$) in a two-doublet version of the Standard Model. A Higgs in the mass range $2\,m_\mu < m_{h^0} < 2\,m_\pi$ has already been excluded in one type of two-Higgs-doublet model (the *Model II* described in Section 2), analysing the decay $\eta \to \pi^0 h^0$ [5]. Here we intend to follow up this study and obtain further constraints in the region $m_{h^0} < 2\,m_\mu$.

Two-Higgs-doublet models are discussed in Section 2, where the different production mechanisms relevant for this study are presented. We use standard Chiral Perturbation Theory (ChPT) techniques to derive the low-energy theorems which fix the hadronic Higgs couplings. Section 3 contains the analysis of experimental data and the constraints obtained. Finally we present our conclusions in Section 4.

2 Two-Higgs-doublet models

The general structure of two-Higgs-doublet models is well known (see ref. [6] for a recent review), so we shall only give here the ingredients we need for the present analysis.

Let us consider two complex $SU(2)_L$ doublet scalars Φ_1 and Φ_2, with hypercharge $Y = 1$. In order to avoid flavour-changing neutral currents (FCNCs), all fermions of a given electric charge should couple to the same Higgs doublet [7]; this can be done in two different ways, resulting in two types of models, namely,

Model I: where only Φ_2^0 couples to fermions, and

Model II: where Φ_1^0 couples only to down-type quarks and charged leptons, while Φ_2^0 couples only to up-type quarks and neutrinos.

(Other choices are possible, treating the quark and lepton couplings asymmetrically.) A particular choice can be made "technically natural" by imposing a set of discrete symmetries ($\Phi_1 \to -\Phi_1$, $\Phi_2 \to \Phi_2$, $\Psi_L \to \Psi_L$ and the appropriate transformation of the right-handed fermion fields).

The spontaneous symmetry breaking of $SU(2)_L \times U(1)_Y$ to $U(1)_{EM}$ is triggered by the vacuum expectation values

$$\langle \Phi_1 \rangle = \begin{pmatrix} 0 \\ \frac{v_1}{\sqrt{2}} \end{pmatrix}, \quad \langle \Phi_2 \rangle = \begin{pmatrix} 0 \\ \frac{v_2}{\sqrt{2}} \end{pmatrix}, \tag{1}$$

where v_1, v_2 can be chosen real and non-negative if the Higgs sector is assumed to be CP-invariant. These vacuum expectation values are related to the W-boson mass through the formula

$$(v_1^2 + v_2^2)^{1/2} \equiv u = \frac{2M_W}{g} \approx 246\,\mathrm{GeV}, \tag{2}$$

leaving one free parameter which is usually taken as

$$\tan\beta = \frac{v_2}{v_1}. \tag{3}$$

In these models there are five physical scalar fields: $H^\pm$, H^0, h^0 and A^0 (A^0 is CP-odd while H^0 and h^0 are CP-even). We are only interested in the lightest neutral scalar

$$h^0 = -\sin\alpha\left(\sqrt{2}\,\mathrm{Re}\,\Phi_1^0 - v_1\right) + \cos\alpha\left(\sqrt{2}\,\mathrm{Re}\,\Phi_2^0 - v_2\right). \tag{4}$$

The mixing angle α is a known function of the parameters of the scalar potential [6].

The quark–Higgs interaction can be written down in the general form

$$\mathcal{L}_{h^0\bar{q}q} = -\frac{h^0}{u}\left\{k_d\,\bar{d}M_d d + k_u\,\bar{u}M_u u\right\}, \tag{5}$$

where M_u and M_d are the diagonal mass matrices for up- and down-type quarks respectively, and the couplings k_u and k_d depend on the model considered. In particular, in the two-Higgs-doublet models introduced above, the couplings of the h^0 neutral scalar are:

$$\begin{aligned} &\textbf{Model I}: && k_d = k_u = \frac{\cos\alpha}{\sin\beta}, \\ &\textbf{Model II}: && k_d = -\frac{\sin\alpha}{\cos\beta}, \quad k_u = \frac{\cos\alpha}{\sin\beta}. \end{aligned} \tag{6}$$

The two models show a completely different pattern. In *Model I*, the Yukawa couplings are identical to the Standard Model ones but for a global factor $\cos\alpha/\sin\beta$, i.e. $g_{h^0\bar{u}u}/g_{h^0\bar{d}d} = M_u/M_d$. *Model II*, however, has different h^0 couplings to up- and down-type quarks, even for $M_u = M_d$.

2.1 Low-energy effective Lagrangian

The hadronic couplings of a light Higgs particle are fixed by low-energy theorems [5, 6, 8, 9, 10], which relate the $P \to P'h^0$ transition with a zero-momentum Higgs to the corresponding $P \to P'$ coupling. The couplings to the octet of lightest pseudoscalar mesons (π, K, η) can be easily worked out, using ChPT techniques.

The lowest-dimensional effective chiral Lagrangian describing the interactions of the pseudoscalar octet is uniquely given [11] by

$$\mathcal{L} = \frac{f^2}{4}\left\{\langle D_\mu U D^\mu U^\dagger\rangle + 2B_0\langle MU^\dagger + UM\rangle\right\}, \tag{7}$$

where $U \equiv \exp\left(-\frac{\sqrt{2}i\Phi}{f}\right)$ is a $SU(3)$ matrix incorporating the octet of pseudoscalar mesons,

$$\Phi(x) \equiv \frac{\vec{\lambda}}{\sqrt{2}}\vec{\varphi} = \begin{pmatrix} \frac{\pi^0}{\sqrt{2}} + \frac{\eta_8}{\sqrt{6}} & \pi^+ & K^+ \\ \pi^- & -\frac{\pi^0}{\sqrt{2}} + \frac{\eta_8}{\sqrt{6}} & K^0 \\ K^- & \bar{K}^0 & -\frac{2\eta_8}{\sqrt{6}} \end{pmatrix}, \tag{8}$$

$f \approx f_\pi = 93.3$ MeV is the pion decay constant at lowest order, and $\langle\rangle$ denote the trace of the corresponding matrix. The second term in (7) is an explicit breaking of chiral symmetry due to the presence of the quark mass matrix $M \equiv \mathrm{diag}\,(m_u, m_d, m_s)$ in the underlying quark Lagrangian. The parameter B_0 relates the squares of the pseudoscalar meson masses to the quark masses,

$$B_0 = \frac{m^2_{\pi^+}}{m_u + m_d} = \frac{m^2_{K^+}}{m_u + m_s} = \frac{m^2_{K^0}}{m_d + m_s}. \tag{9}$$

The electromagnetic interaction is incorporated through the covariant derivative

$$D_\mu U \equiv \partial_\mu U - i|e|\,A_\mu\,[Q, U], \tag{10}$$

where e is the electron charge and Q is a diagonal 3×3 matrix that takes into account the electromagnetic light-quark charges, $Q = \frac{1}{3}\,\mathrm{diag}\,(2, -1, -1)$.

It was shown in ref. [5] that, at lowest order in the momentum expansion, the effective chiral Lagrangian induced by the Yukawa interaction in (5) is given by

$$\mathcal{L}_{h^0} = \frac{f^2}{2}\frac{h^0}{u}\left\{\xi\langle D_\mu U D^\mu U^\dagger\rangle + 3\,\xi B_0\langle MU^\dagger + UM\rangle + B_0\langle(k_d\,A + k_u\,B)\left(MU^\dagger + UM\right)\rangle\right\}, \tag{11}$$

where $A \equiv \mathrm{diag}\,(0,1,1)$ and $B \equiv \mathrm{diag}\,(1,0,0)$. The parameter $\xi \equiv \frac{2}{27}\,(k_d + 2\,k_u)$ collects the information on the heavy quark fields (c, b, t), which remains in the low-energy limit through the Higgs coupling to gluons mediated by one loop of heavy quarks.

We are also interested in the η' couplings; thus we shall introduce the η'-field in our low-energy description by assuming nonet symmetry, which is exact in the large N_c limit (N_c denotes the number of colours), and adding a term that explicitly takes into account the $U(1)_A$ anomaly [12].

In the absence of the $U(1)_A$ anomaly, the singlet η_1 field becomes the ninth Goldstone boson, which is incorporated in the $\Phi(x)$ field as

$$\Phi(x) \equiv \frac{\eta_1}{\sqrt{3}} + \frac{\vec{\lambda}}{\sqrt{2}}\vec{\varphi}. \tag{12}$$

The Lagrangians (7) and (11) describe then the interactions of the whole nonet multiplet.

At first non-trivial order in $1/N_c$, the effect of the $U(1)_A$ anomaly is taken into account by adding the term [12]

$$\mathcal{L}_{U(1)_A} = \frac{f^2}{4}\frac{a}{4\,N_c}(\log U - \log U^\dagger)^2. \tag{13}$$

In the presence of (13) the η_1 field becomes massive even in the chiral limit. After diagonalizing the $\eta_1 - \eta_8$ mass matrix, the physical η and η' fields can be expressed in terms of the $U(3)$ fields η_1 and η_8 as follows

$$\begin{aligned} \eta' &= \cos\theta_P\,\eta_1 + \sin\theta_P\,\eta_8\,, \\ \eta &= -\sin\theta_P\,\eta_1 + \cos\theta_P\,\eta_8\,, \end{aligned} \tag{14}$$

where $\tan\theta_P \approx -1/2\sqrt{2}$. The parameter a is related to the physical meson masses by $a = m_{\eta'}^2 + m_\eta^2 - 2\,m_K^2 \approx 0.73\ \mathrm{GeV}^2$.

The interaction term in (13) induces an additional Higgs coupling to the singlet η_1 field, which is easily obtained by applying the usual low-energy theorems for soft Higgs particles [5]. One gets

$$\mathcal{L}_{h^0\text{-}U(1)_A} = \frac{f^2}{2}\frac{h^0}{u}\frac{a}{2\,N_c}\xi(\log U - \log U^\dagger)^2. \tag{15}$$

Therefore, the interaction between the nine lightest pseudoscalar mesons and the Higgs particle h^0 is described by the Lagrangian given in (11), with the addition of the Lagrangian in (15).

2.2 Light-Higgs decays

A Higgs in the mass range considered in this paper ($m_{h^0} < 2m_\mu$) has only two open decay channels: $h^0 \to e^+e^-$ and $h^0 \to \gamma\gamma$. The decay width into the e^+e^- channel can be easily obtained from the general leptonic Yukawa interaction

$$\mathcal{L}_{h^0\bar{l}l} = -\frac{h^0}{u}\, k_l\, \bar{l} M_l l\,. \tag{16}$$

One gets the result,

$$\Gamma(h^0 \to e^+e^-) = k_l^2\, \frac{m_l^2\, m_{h^0}}{8\,\pi\, u^2} \left(1 - 4\,\frac{m_l^2}{m_{h^0}^2}\right)^{3/2}. \tag{17}$$

In the two-doublet models we are considering here, one has $k_l = k_d$.

The calculation of $\Gamma(h^0 \to \gamma\gamma)$ is slightly more involved, since this transition is generated at the one-loop level. We have distinguished five kinds of contributions to the decay amplitude: $W^\pm$ loops (T_W), $H^\pm$ loops (T_H), (τ, e, μ)-lepton loops (T_L), the contribution from the (c, b, t)-heavy-quark loops (T_Q), and the contribution coming from the (u, d, s)-light-quark loops (T_φ); at the energy we are working, the last contribution is better described in terms of the pseudoscalar meson degrees of freedom ($\pi^\pm$, $K^\pm$). All these contributions are given in the Appendix. The final expression for the $h^0 \to \gamma\gamma$ decay width is then given by

$$\Gamma(h^0 \to \gamma\gamma) = \frac{\alpha^2\, m_{h^0}^3}{256\,\pi^3\, u^2}\, |T_W + T_H + T_L + T_Q + T_\varphi|^2. \tag{18}$$

Since the experimental detection efficiency of such a light Higgs depends strongly on its lifetime, τ_{h^0}, it is interesting to illustrate how τ_{h^0} varies with the parameters of the model. Figures 1a (*Model I*) and 1b (*Model II*) present $c\tau_{h^0}$ as a function of α and β for different values of the Higgs mass. As in the Standard Model the Higgs lifetime increases as the mass decreases and it is infinite for $m_{h^0} = 0$. Figures 2a and 2b show the $\mathrm{Br}(h^0 \to e^+e^-)$ dependence on α and β for various m_{h^0} points. As can be observed, $h^0 \to e^+e^-$ is in general the dominant decay mode, especially at low masses.

2.3 Higgs production at the Z^0 pole

In the models under consideration there are two main Z^0 decays into a neutral Higgs. The first corresponds to the most abundant mechanism in the Standard Model, $Z^0 \to Z^{0*}h^0$, but with a smaller production rate, given by the expression [6]:

$$\frac{\Gamma(Z^0 \to Z^{0*}h^0)}{\Gamma(Z^0 \to Z^{0*}h^0_{SM})} = \sin^2(\beta - \alpha)\,. \tag{19}$$

When the scaling factor $\sin^2(\beta-\alpha)$ tends to zero the coupling $Z^0h^0A^0$ increases and the complementary process $Z^0 \to h^0A^0$ becomes important, if it is kinematically allowed. The corresponding decay width is given by [6]

$$\Gamma(Z^0 \to h^0A^0) = \frac{1}{2}\cos^2(\beta-\alpha)\,\Gamma_{\nu\bar{\nu}}\,\lambda^{3/2}\left(1, \frac{m_{h^0}^2}{m_{Z^0}^2}, \frac{m_{A^0}^2}{m_{Z^0}^2}\right), \tag{20}$$

where $\Gamma_{\nu\bar{\nu}}$ denotes the SM $Z^0 \to \nu_e\bar{\nu}_e$ decay width and $\lambda(x,y,z) = x^2+y^2+z^2-2xy-2yz-2xz$.

2.4 Higgs production through $\eta' \to \eta h^0$

From the Lagrangian given in (11) together with the $U(1)_A$-interaction term in (15), it is straightforward to extract the piece that describes the $h^0\eta\eta'$ coupling. We get

$$\begin{aligned}\mathcal{L}_{\eta\eta' h^0} &= \frac{h^0}{u}\eta\eta'\Big\{(\xi-k_d)\sin\theta_P\cos\theta_P\,[\cos^2\theta_P m_{\eta'}^2 + \sin^2\theta_P m_\eta^2 - \tfrac{2}{3}(m_K^2+\tfrac{1}{2}m_\pi^2)] \\ &\quad + \frac{\sqrt{2}}{6}m_\pi^2\,(k_u-k_d)\,[\sin^2\theta_P - \cos^2\theta_P + \frac{1}{\sqrt{2}}\sin\theta_P\cos\theta_P]\Big\} \\ &= [C_d\,k_d + C_u\,k_u]\;h^0\eta\eta',\end{aligned} \tag{21}$$

with $C_d = 8.20\times10^{-4}$ GeV and $C_u = -1.46\times10^{-4}$ GeV. From this we obtain the following branching ratio,

$$\mathrm{Br}(\eta' \to \eta h^0) = 6.7\times10^{-5}\,(k_d - 0.18\,k_u)^2\,\lambda^{1/2}\left(1, \frac{m_\eta^2}{m_{\eta'}^2}, \frac{m_{h^0}^2}{m_{\eta'}^2}\right). \tag{22}$$

2.5 Higgs production through $\eta \to \pi^0 h^0$

In the SM, η decays always occur through isospin-violating effects. Moreover, the $\eta \to \pi^0h^0$ transition gets an additional suppression factor, because the diagonalization of the kinetic and mass terms of the effective chiral Lagrangian also diagonalizes the lowest-order $PP'h^0$ couplings. It was shown in ref. [5] that these suppression factors no longer hold for general Yukawa interactions with $k_d \neq k_u$. At lowest order in momenta, the $\eta \to \pi^0h^0$ amplitude is given by [5]

$$A(\eta \to \pi^0h^0) = (\cos\theta_P - \sqrt{2}\sin\theta_P)\,\frac{m_\pi^2}{2\sqrt{3}u}\,(k_d-k_u), \tag{23}$$

which leads to the following branching ratio:

$$\mathrm{Br}(\eta \to \pi^0h^0) = 3.3\times10^{-5}\,(k_d-k_u)^2\,\lambda^{1/2}\left(1, \frac{m_\pi^2}{m_\eta^2}, \frac{m_{h^0}^2}{m_\eta^2}\right). \tag{24}$$

In *Model I*, $k_d = k_u$ and one therefore needs to go to the next order in the momentum expansion to get a non-zero amplitude. The resulting branching ratio is easily obtained [5], by rescaling the SM result [9] with the Yukawa factor k_d $(= k_u)$. One gets, of course, a much smaller rate in this case [5]:

$$\mathrm{Br}(\eta \to \pi^0 h^0)_{Mod.I} = 6 \times 10^{-7}\, k_d^2\, \lambda^{1/2}\left(1, \frac{m_\pi^2}{m_\eta^2}, \frac{m_{h^0}^2}{m_\eta^2}\right). \tag{25}$$

2.6 Higgs production through $\pi \to e\nu h^0$

The W-exchange transition $\pi \to e\bar{\nu}_e$ is described by the effective Lagrangian

$$\mathcal{L}_W = -\sqrt{2}\, G_F \cos\theta_C\, \bar{e}\gamma^\mu(1-\gamma_5)\nu_e\, (L_\mu)_{21} + h.c., \tag{26}$$

where $(L_\mu)_{21}$ denotes the (2,1) element of the 3×3 matrix

$$L^\mu \equiv \frac{1}{2}(V-A)^\mu = -i\frac{f_\pi^2}{2}\, U^\dagger D^\mu U = -\frac{f_\pi}{\sqrt{2}}\, D^\mu \Phi + \cdots, \tag{27}$$

corresponding to the hadronic left-handed current, θ_C is the Cabibbo mixing angle, and G_F the Fermi constant.

The direct $\pi \to e\bar{\nu}_e h^0$ transition amplitude, generated by the h^0-coupling to the W field,

$$\mathcal{L}_{h^0 W^+ W^-} \equiv \frac{h^0}{u}\, \sin(\beta-\alpha)\, M_W\, \frac{\partial \mathcal{L}}{\partial M_W} \tag{28}$$

($\mathcal{L}$ denotes the underlying weak Lagrangian with the h^0-field set to zero), can be easily obtained from $\mathcal{L}_W$ [10]. Since $G_F \sim M_W^{-2}$, the resulting vertex is given by

$$\mathcal{L}_{h^0 \pi e \nu} = -\frac{2h^0}{u}\, [\sin(\beta-\alpha) - \xi]\, G_F\, f_\pi\, \cos\theta_C D_\mu \pi^-\, \bar{e}\gamma^\mu(1-\gamma_5)\nu_e + h.c. \tag{29}$$

This effective Lagrangian corresponds to the contribution coming from diagram (a) in Fig. 3. In addition, one should include the contributions from the other two diagrams [(b) and (c)] where the light Higgs couples to the electron or to the pion fields. If the electron mass is neglected, diagrams (b) and (c) give a zero contribution; the decay width is then given by the formula

$$\Gamma(\pi^\pm \to h^0 e^\pm \nu_e) = \frac{\sqrt{2}\, G_F^3\, f_\pi^2 \cos^2\theta_C}{192\,\pi^3}\, m_\pi^5\, f(m_{h^0}^2/m_\pi^2)\, [\sin(\beta-\alpha) - \xi]^2, \tag{30}$$

where $f(x) = (1-x^2)(1-8x+x^2) - 12x^2 \log x$. This width leads to the following branching ratio:

$$\mathrm{Br}(\pi^\pm \to h^0 e^\pm \nu_e) = 6.5 \times 10^{-9}\, f(m_{h^0}^2/m_\pi^2)\, [\sin(\beta-\alpha) - \xi]^2. \tag{31}$$

3 Experimental results

3.1 Around the Z^0 pole

LEP experiments have looked for a very light Higgs in the framework of the Minimal Supersymmetric extension of the Standard Model (MSSM) [13]. The scalar sector of the MSSM is just a particular case of our *Model II*, with additional (supersymmetric) constraints on the parameters. Therefore, it is not difficult to work out the LEP information in order to transform it into constraints on more general two-Higgs-doublet models. The LEP limits are expressed as a function of the two free parameters in the MSSM: $\tan\beta$ and m_{h^0}. Since experimentally the detection efficiency depends on the Higgs mass and lifetime (τ_{h^0}), it is possible to transform the excluded areas in the $(\tan\beta, m_{h^0})$ plane into non-allowed zones in the (τ_{h^0}, m_{h^0}) space. The next step is to calculate the excluded areas in the (α, β, m_{h^0}) space, since for given α and β values the lifetime is fixed. The results obtained at the 90% C.L. are plotted in (α, β) planes for different values of the Higgs mass in Figs. 4a (*Model I*) and 4b (*Model II*). As can be observed the excluded areas are largest for $m_{h^0} = 0$, where the experimental detection efficiency is maximum and the sensitivity is only limited by the production cross section.

3.2 η' decays

Beam-dump experiments have been used to look for Weakly Interacting Neutral Particles (WINPs). The dump, placed behind the target, is used to absorb all strongly or electromagnetically interacting particles, produced in the primary reaction, and therefore only WINPs traverse it. A detector placed behind the dump is intended to reveal the decays or collisions of such WINPs. In the present study we reanalyse data from an experiment carried out at Fermilab [14], extending the work reported in ref. [15], where the method used is explained in detail. A 400 GeV/c proton beam was incident on an iron target, with a total number of interacting projectiles $N_p = 2.8 \times 10^{13}$. The experiment did not find any evidence of WINPs decaying into charged particles in a certain region behind the dump and this lack of signal was used to set limits on WINPs. Applying that result to our case, the number of expected Higgs events is given by the expression

$$N_{h^0} = N_p n_{\eta'} \epsilon \, \mathrm{Br}(\eta' \to \eta h^0) \, D_{h^0} \, \mathrm{Br}(h^0 \to e^+e^-), \tag{32}$$

where $n_{\eta'}$ is the number of η' particles produced per collision. The factor ϵ includes the detector acceptance and Higgs reconstruction efficiency as calculated in ref. [15], and D_{h^0} is the probability that the Higgs disintegrates inside the experimental

sensitive volume; it is given by

$$D_{h^0} = \exp\left(-\frac{L_1}{c\beta_{h^0}\tau_{h^0}\gamma_{h^0}}\right)\left[1-\exp\left(-\frac{L_2-L_1}{c\beta_{h^0}\tau_{h^0}\gamma_{h^0}}\right)\right], \tag{33}$$

where $L_{1(2)}$ is the distance from the target to the front (back) edge of the sensitive volume along the Higgs trajectory. The second term in parenthesis reflects the finite length of the vacuum volume. Since no WINP candidates were observed in the experiment under consideration, limits on $\mathrm{Br}(\eta' \to \eta h^0)$ can be established and by comparing them with the theoretical calculation (22) certain values of the model parameters can be excluded. For a SM Higgs the number of expected Higgs events (N_{h^0}) given in expression (32) is unique for a given mass. Conversely, in the case of two-Higgs-doublet models, N_{h^0}, and therefore the limits obtained, depends not only on the mass but, in addition, on the α and β angles. Figs. 5a and 5b show the regions excluded at the 90% C.L. in the (α, β) plane for different values of the Higgs mass. As can be seen the areas excluded by this analysis are quite substantial especially around $m_{h^0} = 50$ MeV. No constraints can be derived for $m_{h^0} < 2m_e$ since such a light Higgs would not be seen in the experimental set-up considered here. The excluded areas decrease as the mass increases, since the lifetime gets shorter and therefore the number of Higgs particles reaching the sensitive volume in the experiment also decreases.

3.3 η analysis

Data from an experiment carried out at the Rutherford Laboratory [16] have been used to extract limits on Higgs produced through η decay. The η's were produced through the reaction $\pi^- p \to \eta n$ using an incident pion beam with 718 MeV energy, just 33 MeV above the η production threshold. The beam was incident on a cylindrical hydrogen target 34 cm long and 4 cm wide [17]. The neutron produced in the reaction was used to tag the η particle. The experiment studied several η decays and in particular looked for the process $\eta \to \pi^0 e^+ e^-$. In this search the electrons were identified with some Cherenkov counters, and their trajectories, reconstructed with a tracking system, were required to have a common origin inside the hydrogen target. No significant signal was found and a limit $\Gamma(\eta \to \pi^0 e^+ e^-) < 4.5 \times 10^{-5}$ was established at 90% C.L. In the present study we want to apply this limit to a Higgs produced in the reaction $\eta \to \pi^0 h^0$, $h^0 \to e^+ e^-$. Such a process would have been seen in the experiment under consideration if the Higgs had decayed inside the hydrogen target. Therefore it is necessary to calculate the probability P_d that the Higgs would have decayed inside the target for its different masses and lifetimes. This was done with a Monte Carlo program where the η was generated randomly along the target. In addition the maximum momentum allowed by kinematics was assigned to the η

in the direction perpendicular to the beam axis. This choice was made in order to be conservative in our estimation. Once the η was generated Higgses with different masses and lifetimes were produced, through the decay under consideration, and their decayed point was simulated. The probability P_d obtained in this way was then used to rescale the limit on the branching ratio according to $\Gamma_h = \Gamma_{exp}/P_d$. The values obtained in this way were then compared with the theoretical expression in eqs. (24) and (25). The areas excluded at the 90% C.L. in the (α,β) plane can be seen in Figs. 6a and 6b for *Models I* and *II* respectively.

3.4 Pion decay

Two experiments have been used to deduce limits on the SM Higgs based on the decay $\pi \to e\nu h^0$ [18, 19, 20]. The most complete analysis has been performed by the SINDRUM Collaboration, looking for the decay $\pi \to e\nu h^0$ with subsequent decay $h^0 \to e^+e^-$. Limits on such a process were given as a function of the Higgs mass and lifetime in ref. [19]. In the present study we have considered those general constraints and transformed them into light-Higgs limits in the context of two-Higgs-doublet models. If the α and β angles are known, the lifetime is fixed and therefore limits on the branching ratio $\mathrm{Br}(\pi \to e\nu h^0)$ can be obtained, from the SINDRUM results. Then, excluded regions in the (α, β, m_{h^0}) space can be calculated, by comparing with its theoretical value (31). The results obtained at the 90% C.L. from this analysis are presented in Figs. 7a and 7b, in (α, β) planes for different Higgs masses. The largest excluded region corresponds also to a Higgs mass around 50 MeV. The decay under study is not kinematically allowed for $m_{h^0} > m_\pi - m_e$ and therefore no limits can be derived for that region.

4 Summary

We have studied the present experimental constraints on a possible light scalar Higgs ($m_{h^0} < 2m_\mu$), in the context of two-Higgs-doublet models. The light Higgs production channels $Z^0 \to Z^{0*}h^0$, $\eta' \to \eta h^0$, $\eta \to \pi^0 h^0$, and $\pi \to e\nu h^0$ have been considered. We have applied standard ChPT techniques to derive the low-energy theorems which fix the hadronic Higgs couplings. Using published results from Higgs searches at LEP, fixed-target experiments and pion decay analyses, we have been able to set strong limits on such a light scalar. These limits are shown in Figs. 4, 5, 6 and 7.

Figures 8a and 8b show the final areas excluded at the 90% C.L., taking into account the four different approaches considered in this work. For a zero-mass Higgs only limits derived from LEP results can be used. For higher masses, where

the decay $h^0 \to e^+e^-$ is allowed, the most constraining limits come from the $\eta' \to \eta h^0$ analysis, especially at intermediate masses $m_{h^0} \approx 50$ MeV. The bounds provided by the four processes turn out to be quite complementary, allowing us to exclude a large area in the parameter-space of both models.

Acknowledgements

We would like to thank Marcel Bonapart for his very useful contribution in providing the program for the calculation of excluded areas, and Fabio Zwirner for reading the manuscript. The work of two uf us (A.P. and J.P.) has been supported in part by CICYT, Spain, under grant No. AEN90-0040. J.P. is indebted to the Spanish Ministerio de Educación y Ciencia for a fellowship.

Appendix: The $h^0 \to \gamma\gamma$ decay amplitude

In this section we give the different loop contributions to the $h^0 \to \gamma\gamma$ decay width in eq. (18). Following ref. [6], we introduce the kinematical functions:

$$\begin{aligned} F_0(x) &\equiv x\,[1 - x\,g(x)], \\ F_{1/2}(x) &\equiv -2x\,[1 + (1 - x)\,g(x)]\,, \\ F_1(x) &\equiv 2 + 3x\,[1 + (2 - x)\,g(x)], \end{aligned} \tag{A.1}$$

corresponding to loops with intermediate particles of spin 0, 1/2, and 1, respectively. Here

$$g(x) \equiv \begin{cases} \left[\arcsin\left(\frac{1}{\sqrt{x}}\right)\right]^2 & (x \geq 1), \\ -\frac{1}{4}\left[\log\left(\frac{1+\sqrt{1-x}}{1-\sqrt{1-x}}\right) - i\pi\right]^2 & (x < 1), \end{cases} \tag{A.2}$$

and $x \equiv 4m^2/m_{h^0}^2$, where m denotes the mass of the particle running along the loop. When x becomes large, i.e. when the particle in the loop is much heavier than h^0, these loop functions approach the limits:

$$F_0(x) \to -\frac{1}{3}\,, \qquad F_{1/2}(x) \to -\frac{4}{3}\,, \qquad F_1(x) \to 7\,. \tag{A.3}$$

The amplitude contribution coming from the W loops is [6]

$$T_W \;=\; \sin(\beta-\alpha)\,F_1(x_W) \;\approx\; 7\,\sin(\beta-\alpha)\,, \tag{A.4}$$

where we have used the fact that $x_W \equiv 4M_W^2/m_{h^0}^2 >> 1$ for the range of light-Higgs masses we are interested in.

For the charged-Higgs loop-amplitude contribution one gets the result [6]:

$$T_H = \left[\sin(\beta-\alpha) + \frac{\cos 2\beta \, \sin(\alpha+\beta)}{2\cos^2\theta_W}\right] \frac{M_W^2}{M_{H^\pm}^2} F_0(x_{H^\pm}) . \qquad \text{(A.5)}$$

The mass of the charged scalar $H^\pm$ has a model-independent lower bound of about 40 GeV [21]; therefore, for a very light h^0, $F_0(x_{H^\pm}) \approx -1/3$. This contribution is then much smaller than T_W, except for very small regions of the parameter space where $\sin(\beta-\alpha) << 1$. Variations of $M_{H^\pm}$ in the range 40–1000 GeV have a negligible effect on our results.

The lepton (e, μ, τ)-loop contributions are given by [6]

$$T_L = k_l \left[F_{1/2}(x_\tau) + F_{1/2}(x_\mu) + F_{1/2}(x_e)\right] \approx k_l \left[-\frac{4}{3} + F_{1/2}(x_\mu) + F_{1/2}(x_e)\right], \qquad \text{(A.6)}$$

while for the contributions coming from the heavy-quark loops one gets the result:

$$T_Q = N_c \left\{\frac{4}{9} k_u \left[F_{1/2}(x_t) + F_{1/2}(x_c)\right] + \frac{1}{9} k_d \, F_{1/2}(x_b)\right\} \approx -\frac{32}{9} k_u - \frac{4}{9} k_d . \qquad \text{(A.7)}$$

At the energy we are interested in, the contribution from the light-quark (u, d, s) loops is better described in terms of mesonic degrees of freedom. In the ChPT formalism introduced in Section 2, this contribution is given by charged kaon and pion loops,

$$T_\varphi = T_\pi + T_K . \qquad \text{(A.8)}$$

The calculation of these chiral loops is rather straightforward. The result we have obtained can be written as:

$$\begin{aligned} T_\pi &= \left[2\xi\left(1 + \frac{4}{x_\pi}\right) + k_u + k_d\right] \frac{1}{4} F_0(x_\pi) , \\ T_K &= \left[2\xi\left(1 + \frac{4}{x_K}\right) + k_u\,\delta + k_d\,(2-\delta)\right] \frac{1}{4} F_0(x_K) , \end{aligned} \qquad \text{(A.9)}$$

where $\xi = \frac{2}{27}(k_d + 2k_u)$, $\delta = m_\pi^2/m_K^2$, $x_\pi = 4m_\pi^2/m_{h^0}^2$, and $x_K = 4m_K^2/m_{h^0}^2$. For a very light scalar, i.e. $x_K > x_\pi >> 1$, and making the approximation $\delta \approx 0$, the total contribution from the light pseudoscalar-meson loops reduces to the simple formula:

$$T_\varphi \approx -0.14\, k_u - 0.27\, k_d . \qquad \text{(A.10)}$$

References

[1] ALEPH Collaboration, Contribution to the Aspen, La Thuile and Moriond conferences (Winter 1991), CERN preprint CERN-PPE/91-19 (1991);

DELPHI Collaboration, P. Abreu et al., "Search for Neutral Higgs Particles in Z^0 decays", CERN preprint CERN-PPE/91-132;

L3 Collaboration, B. Adeva et al., Phys. Lett. **B257** (1991) 450;

OPAL Collaboration, M.Z. Akrawy et al, Phys. Lett. **B253** (1991) 511;

M. Davier, "Searches at LEP", Rapporteur's talk at the LP-HEP91 Conference, Geneva, July 1991.

[2] S. Dimopoulos and H. Georgi, Nucl. Phys. **B193** (1981) 150.

[3] R.D. Peccei and H.R. Quinn, Phys. Rev. Lett. **38** (1977) 1440; Phys. Rev. **D16** (1977) 1791.

[4] T.D. Lee, Phys. Rev. **D8** (1973) 1226;

S. Weinberg, Phys. Rev. Lett. **37** (1976) 657.

[5] J. Prades and A. Pich, Phys. Lett. **B245** (1990) 117.

[6] J.F. Gunion, H.E. Haber, G.L. Kane and S. Dawson, "The Higgs Hunter's Guide", Frontiers in Physics Lecture Note Series, Addison-Wesley Publishing Company, 1990.

[7] S. Glashow and S. Weinberg, Phys. Rev. **D15** (1977) 1958.

[8] J. Ellis, M.K. Gaillard and D.V. Nanopoulos, Nucl. Phys. **B106** (1976) 292;

A.I. Vainshtein, M.B. Voloshin, V.I. Zakharov and M.A. Shifman, Sov. J. Nucl. Phys. **30** (1979) 711;

A.I. Vainshtein, V.I. Zakharov and M.A. Shifman, Sov. Phys. Usp. **23** (1980) 429;

M.B. Voloshin, Sov. J. Nucl. Phys. **44** (1986) 478 and **45** (1987) 122;

R. Ruskov, Phys. Lett. **B187** (1987) 165.

B. Grinstein, L. Hall and L. Randall, Phys. Lett. **B211** (1988) 363;

R.S. Chivukula and A.V. Manohar, Phys. Lett. **B207** (1988) 86 [E: **B217** (1989) 568];

R.S. Chivukula, A. Cohen, H. Georgi, B. Grinstein and A.V. Manohar, Ann. Phys. **192** (1989) 93;

R.S. Chivukula, A. Cohen, H. Georgi and A.V. Manohar, Phys. Lett. **B222** (1989) 258.

[9] H. Leutwyler and M.A. Shifman, Phys. Lett. **B221** (1989) 384; Nucl. Phys. **B343** (1990) 369.

[10] S. Dawson, Phys. Lett. **B222** (1989) 143.

[11] J. Gasser and H. Leutwyler, Nucl. Phys. **B250** (1985) 465.

[12] E. Witten, Nucl. Phys. **B156** (1979) 269;

G. Veneziano, Nucl. Phys. **159** (1979) 213;

P. Di Vecchia, Phys. Lett. **85B** (1979) 357.

[13] ALEPH Collaboration, D. Decamp et al., "Search for the neutral Higgs bosons of the MSSM and other two-doublet models", CERN preprint CERN-PPE/91-111 (1991); Phys. Lett. **B236** (1990) 233 and **B245** (1990) 289;

DELPHI Collaboration, P. Abreu et al., Z. Phys. **C51** (1991) 25;

L3 Collaboration, B. Adeva et al., Phys. Lett. **B251** (1990) 311;

OPAL Collaboration, M.Z. Akrawy et al., Z. Phys. **C49** (1991) 1.

[14] D.J. Bechis et al., Phys. Rev. Lett. **40** (1978) 602.

[15] P. Yepes, Phys. Lett. **B229** (1989) 156; Mod. Phys. Lett. **A5** (1990) 183.

[16] M.R. Jane et al., Phys. Lett. **B59** (1975) 99 and **B48** (1974) 260.

[17] J. Kirkby, private communication.

[18] P. Yepes, Phys. Lett. **B227** (1989) 182.

[19] R. Eichler et al., Phys. Lett. **B175** (1986) 101.

[20] S. Egli et al., Phys. Lett. **B222** (1989) 533.

[21] L3 Collaboration, B. Adeva et al., Phys. Lett. **B252** (1990) 511;

OPAL Collaboration, M.Z. Akrawy et al., Phys. Lett. **B242** (1990) 299.

h^0 Lifetime

Model I

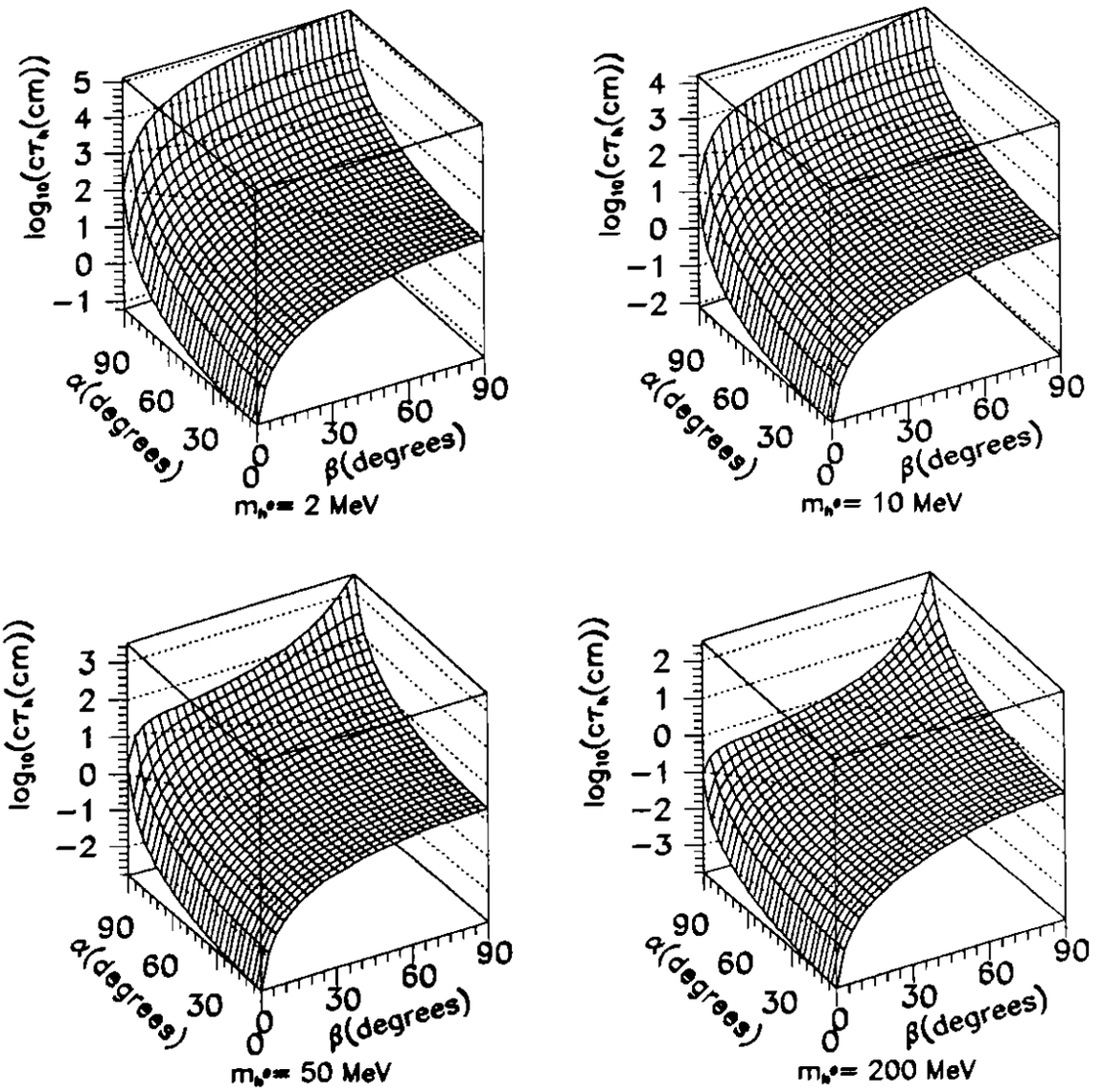

Figure 1.a: Higgs lifetime dependence on the α and β angles for different masses ($m_{h^0} = 2, 10, 50, 200$ MeV) in *Model I*

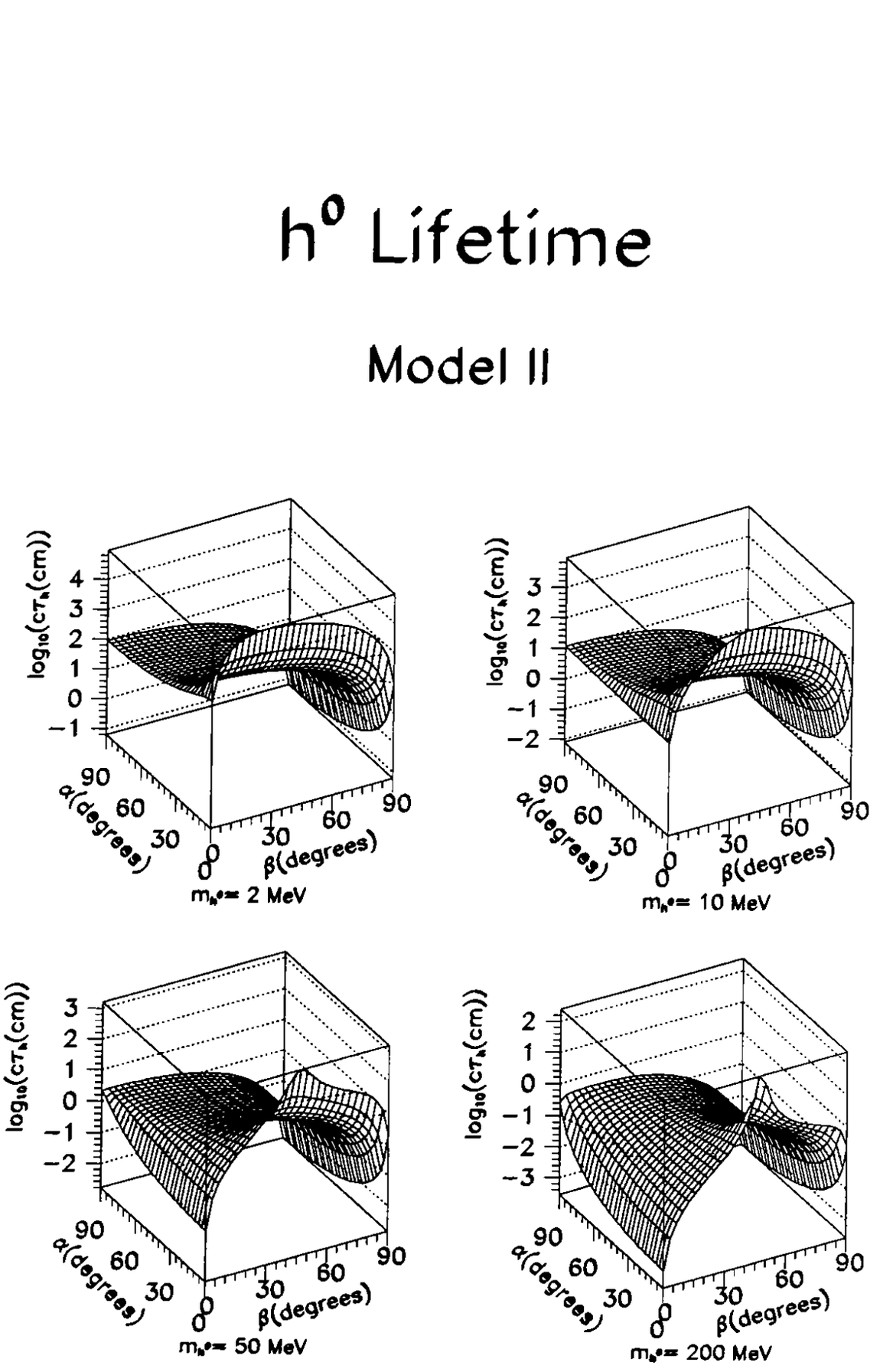

Figure 1.b: Higgs lifetime dependence on the α and β angles for different masses ($m_{h^0} = 2, 10, 50, 200$ MeV) in *Model II*

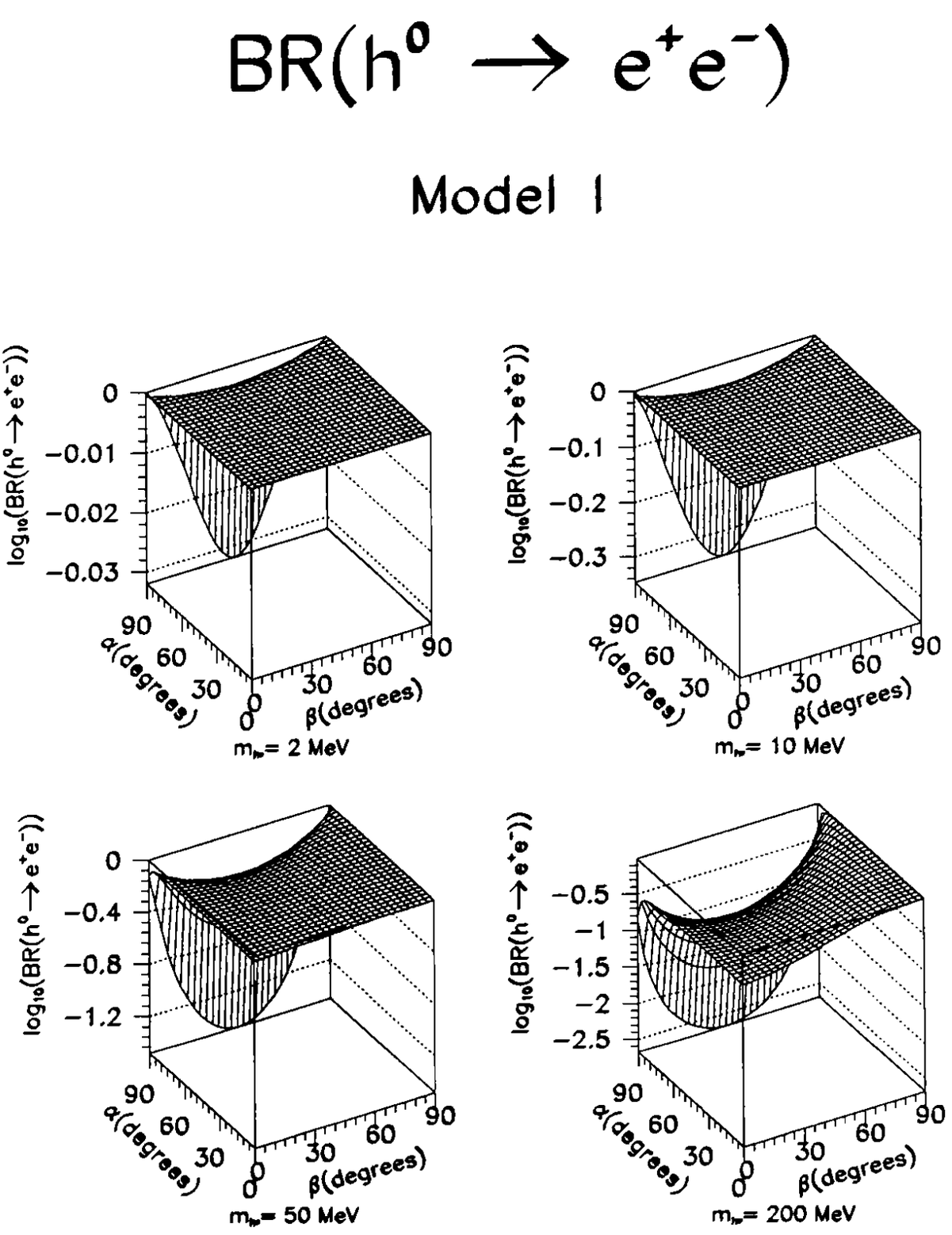

Figure 2.a: BR($h^0 \rightarrow e^+e^-$) dependence on the α and β angles for different masses ($m_{h^0} = 2, 10, 50, 200$ MeV) in *Model I*

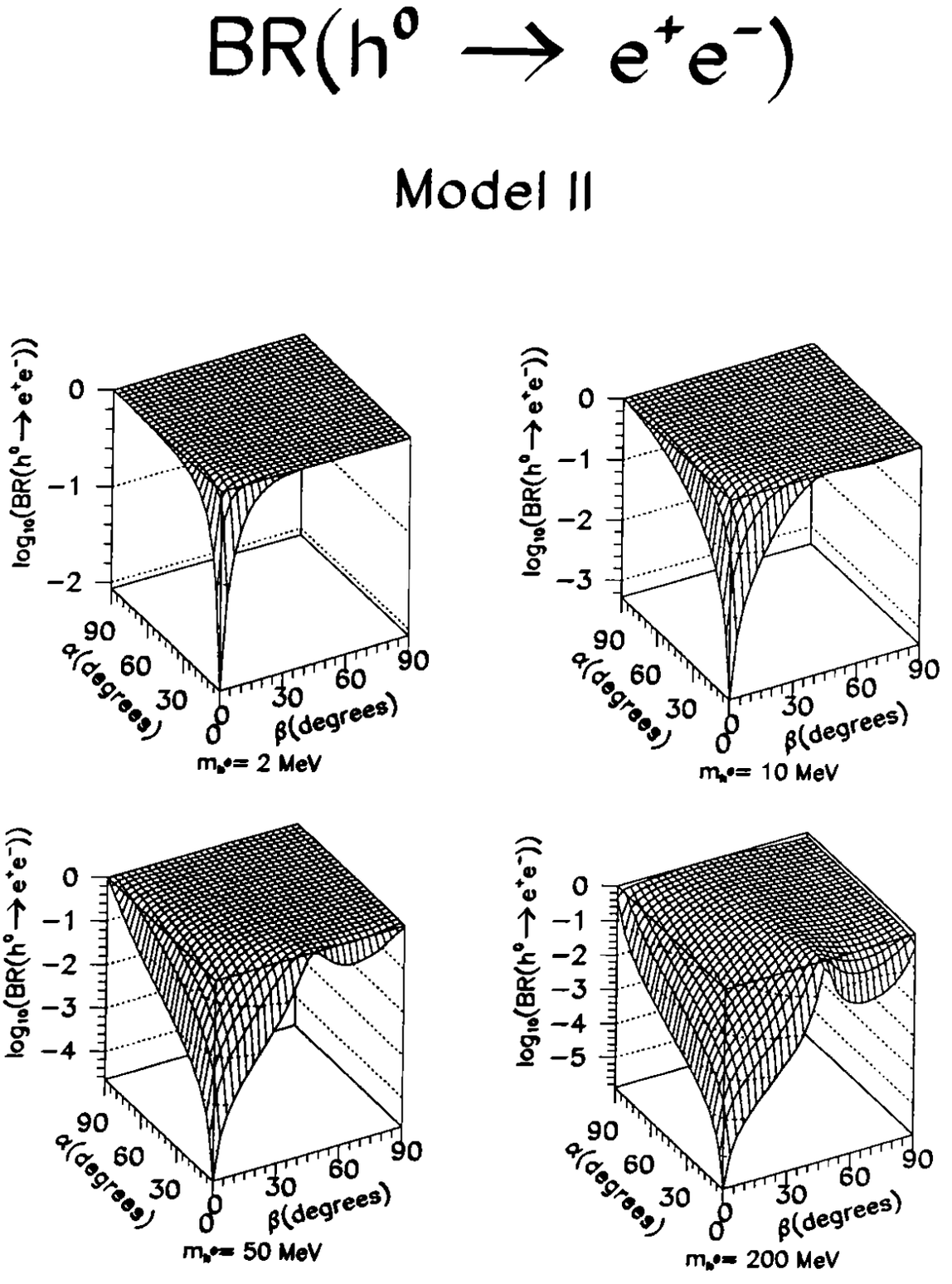

Figure 2.b: BR($h^0 \to e^+e^-$) dependence on the α and β angles for different masses ($m_{h^0} = 2, 10, 50, 200$ MeV) in *Model II*

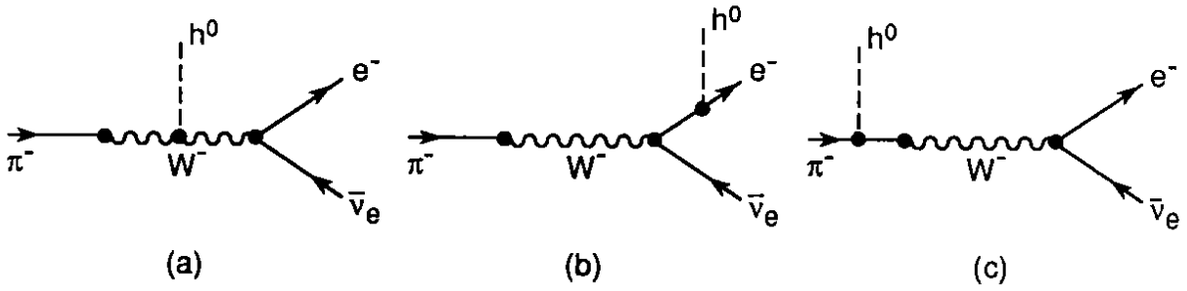

Figure 3: Feynman diagrams contributing to the decay $\pi^- \to e^- \bar{\nu}_e h^0$

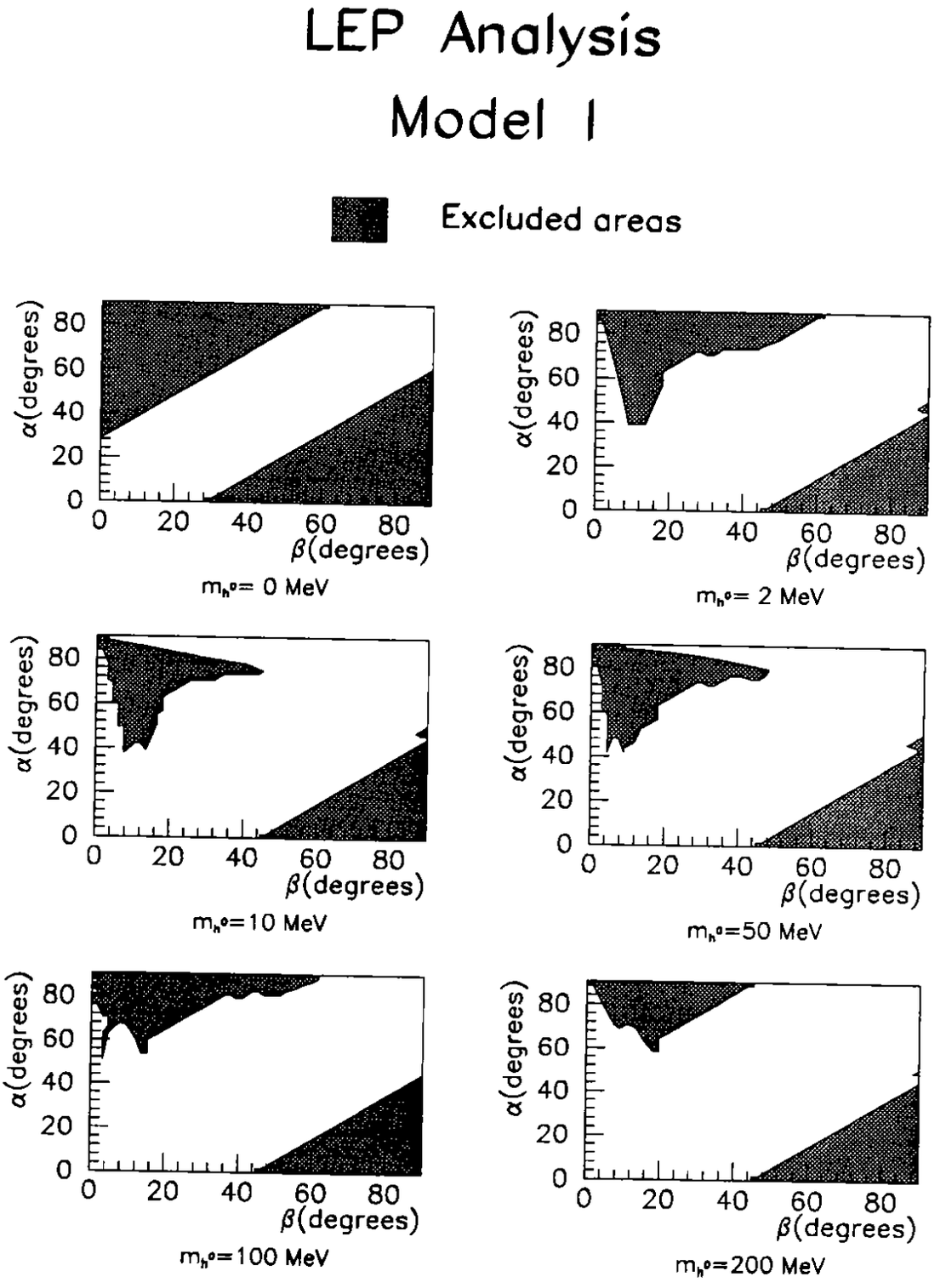

Figure 4.a: Areas in the (α, β) plane excluded at 90% C.L. by LEP for different Higgs masses ($m_{h^0} = 0, 2, 10, 50, 100, 200$ MeV) in *Model I*

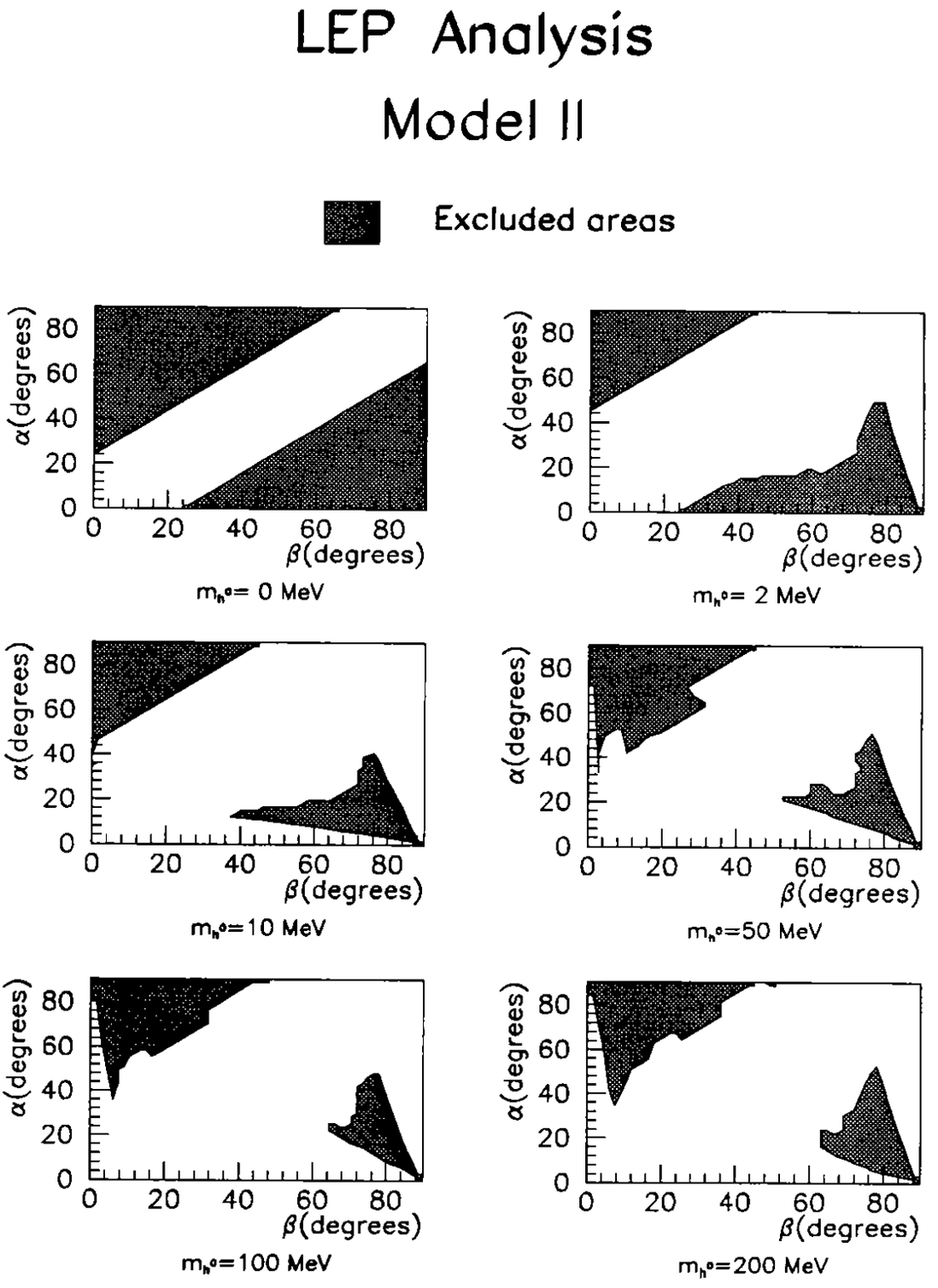

Figure 4.b: Areas in the (α, β) plane excluded at 90% C.L. by LEP for different Higgs masses ($m_{h^0} = 0, 2, 10, 50, 100, 200$ MeV) in *Model II*

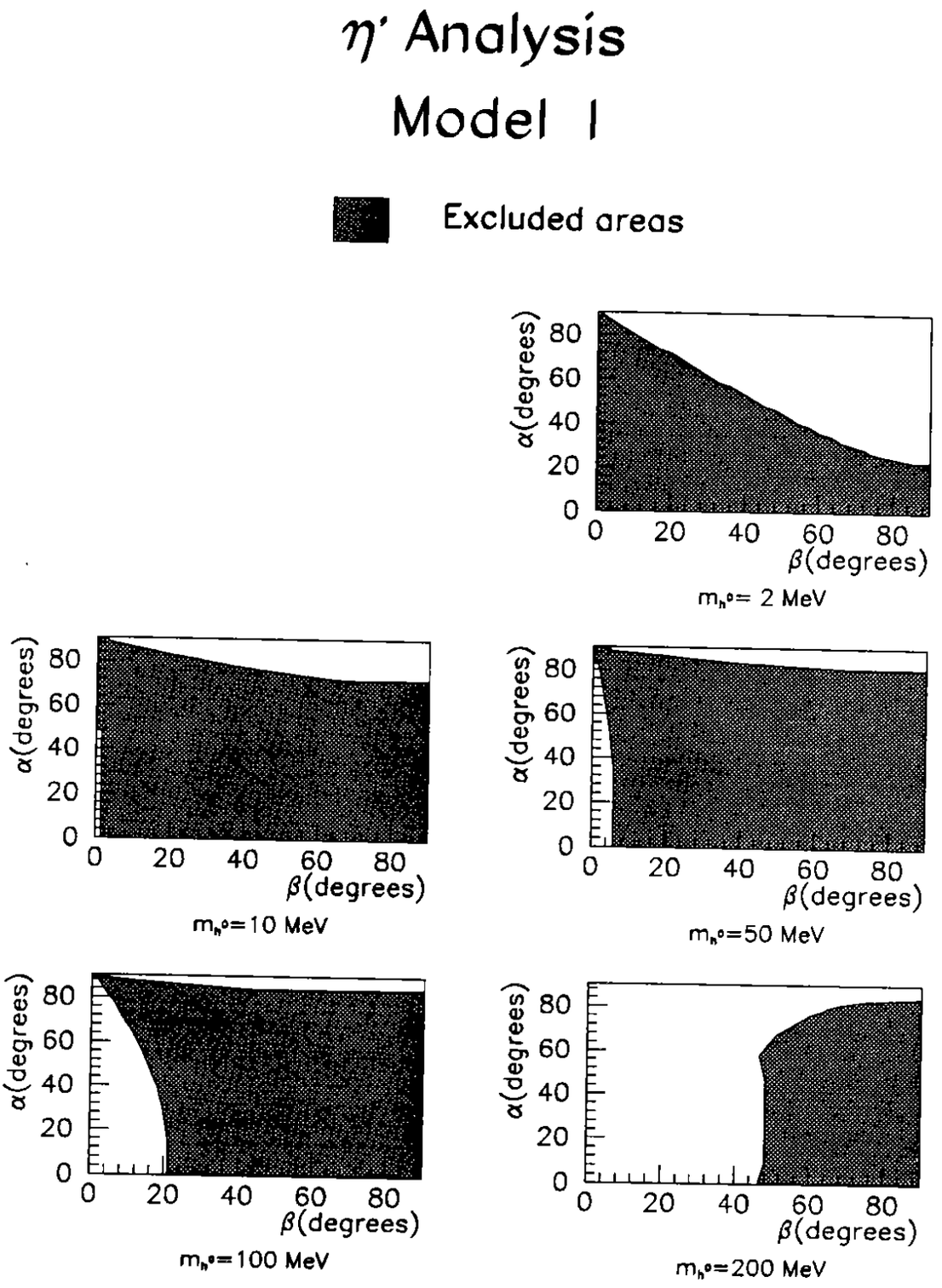

Figure 5.a: Areas in the (α, β) plane excluded at 90% C.L. by the η' analysis for different Higgs masses ($m_{h^0} = 2, 10, 50, 100, 200$ MeV) in *Model I*

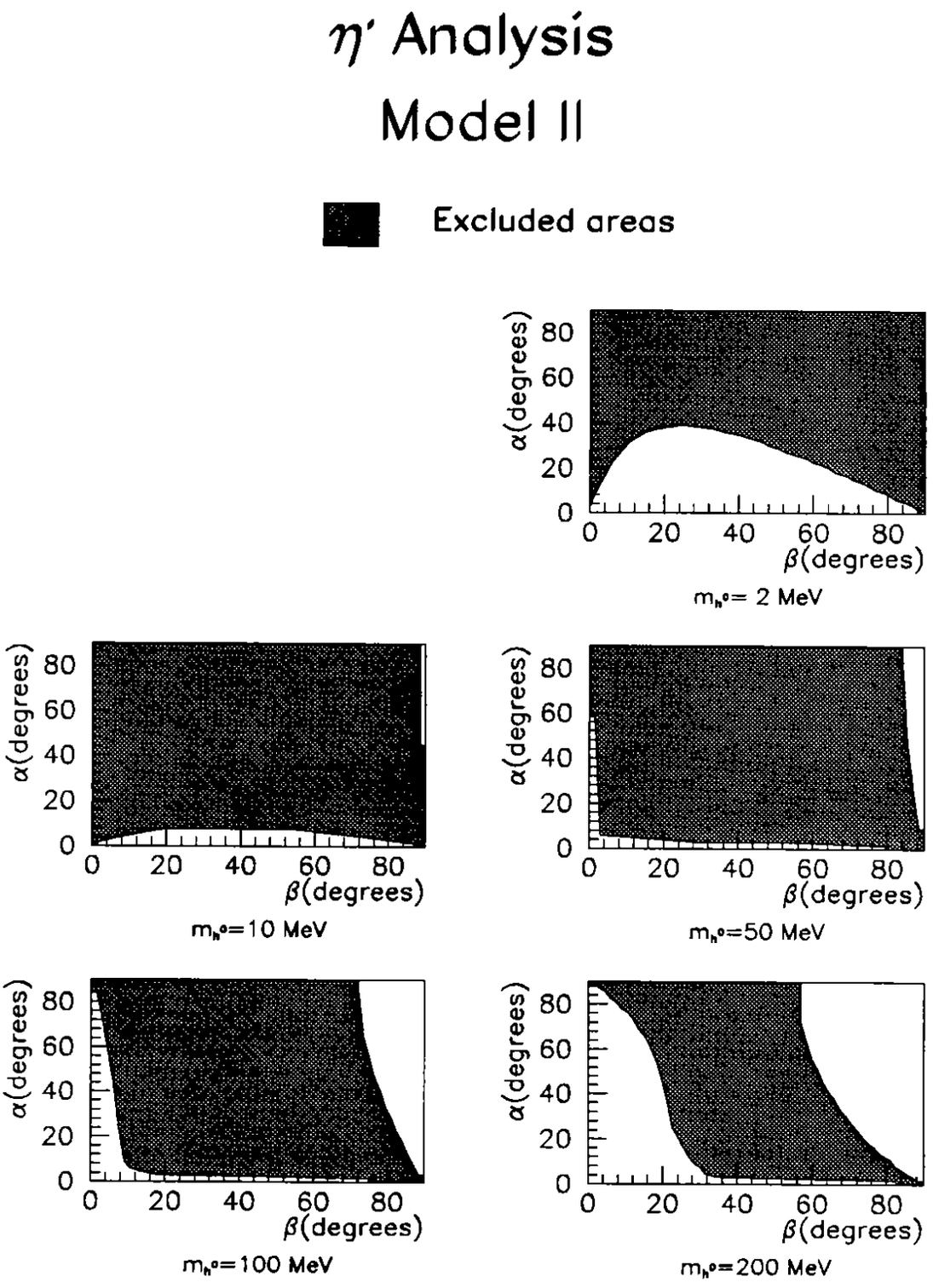

Figure 5.b: Areas in the (α, β) plane excluded at 90% C.L. by the η' analysis for different Higgs masses ($m_{h^0} = 2, 10, 50, 100, 200$ MeV) in *Model II*

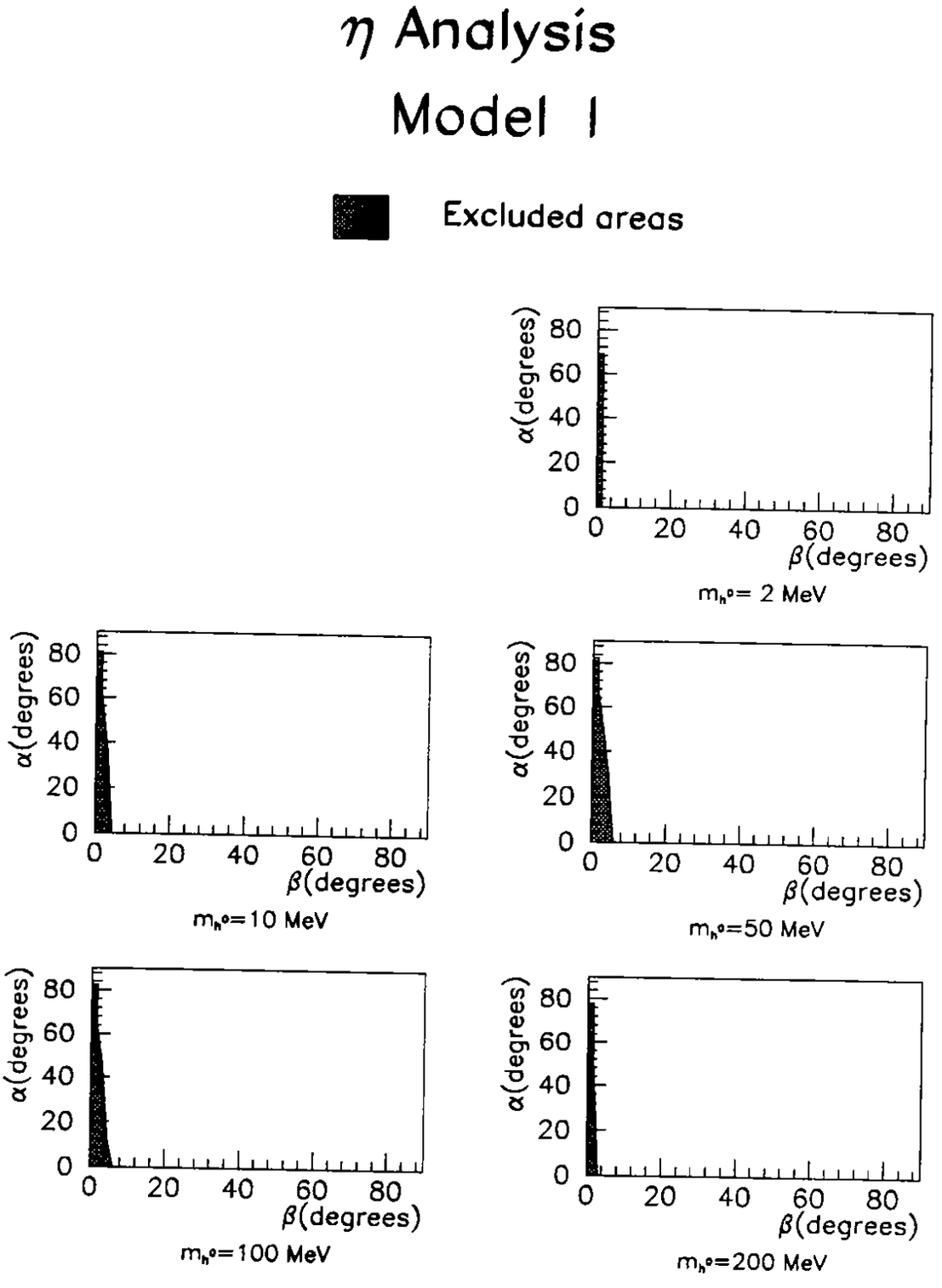

Figure 6.a: Areas in the (α, β) plane excluded at 90% C.L. by the η analysis for different Higgs masses ($m_{h^0} = 2, 10, 50, 100, 200$ MeV) in *Model I*

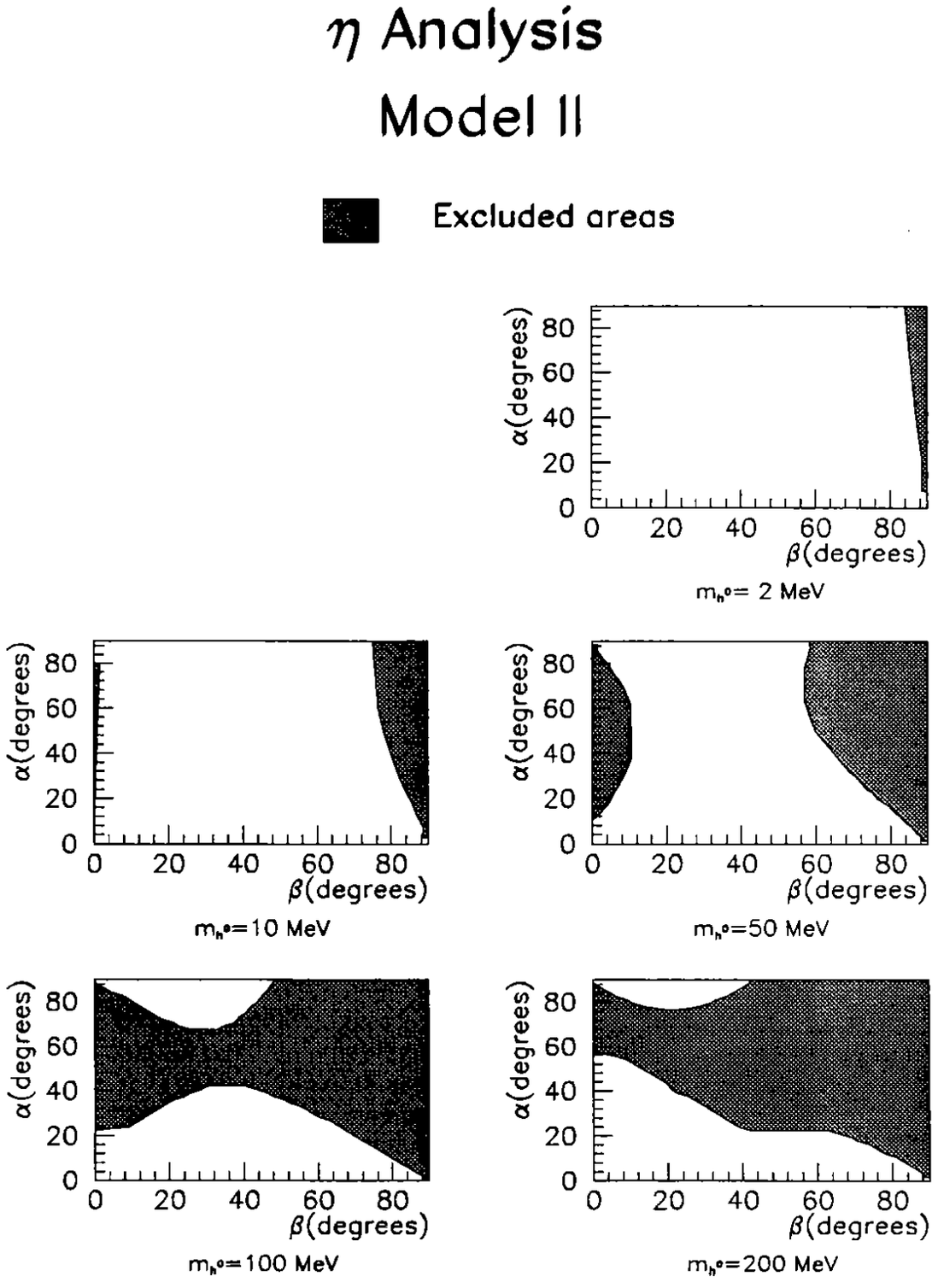

Figure 6.b: Areas in the (α, β) plane excluded at 90% C.L. by the η analysis for different Higgs masses ($m_{h^0} = 2, 10, 50, 100, 200$ MeV) in *Model II*

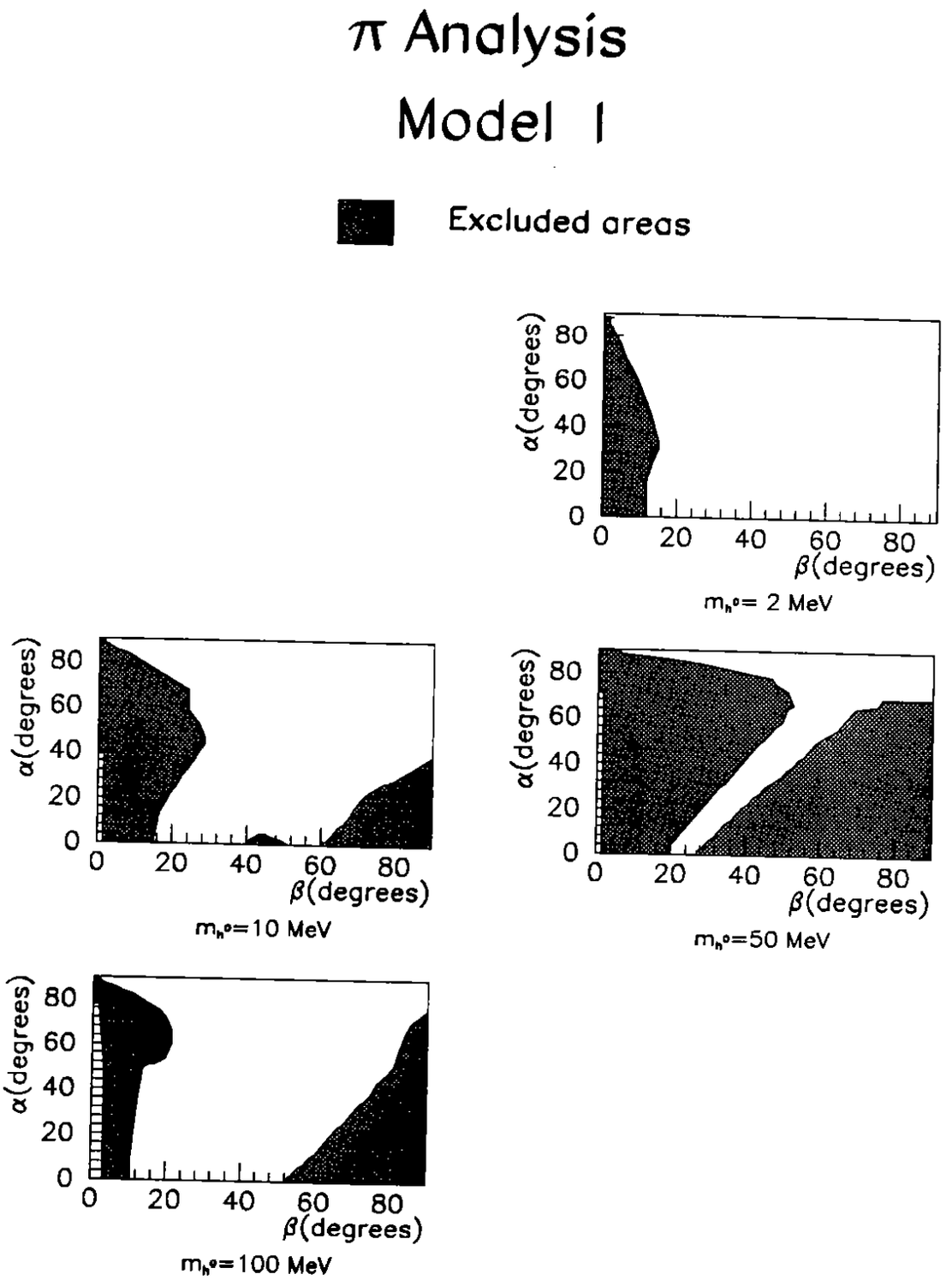

Figure 7.a: Areas in the (α, β) plane excluded at 90% C.L. by the π analysis for different Higgs masses ($m_{h^0} = 2, 10, 50, 100$ MeV) in *Model I*

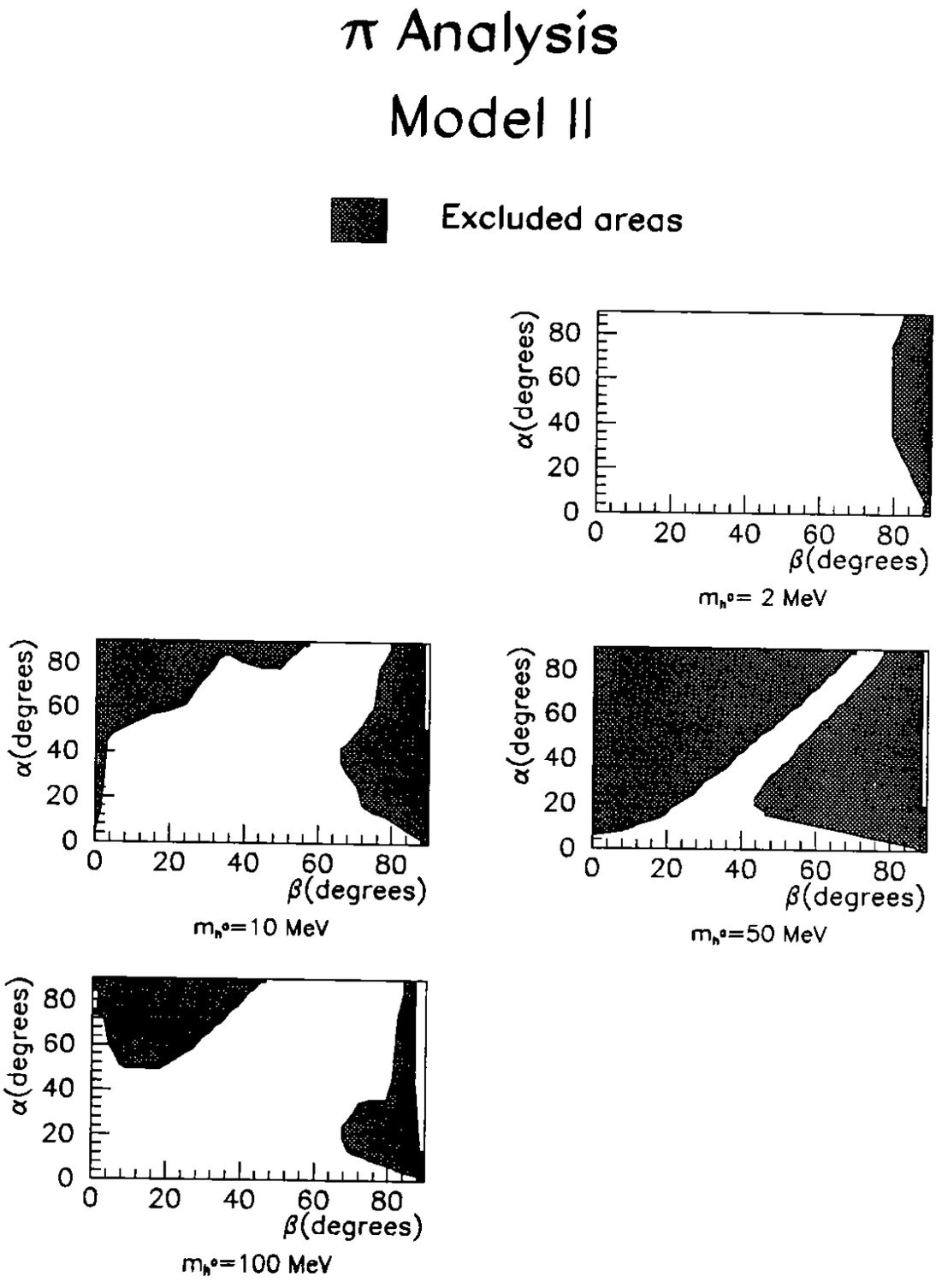

Figure 7.b: Areas in the (α, β) plane excluded at 90% C.L. by the π analysis for different Higgs masses ($m_{h^0} = 2, 10, 50, 100$ MeV) in *Model II*

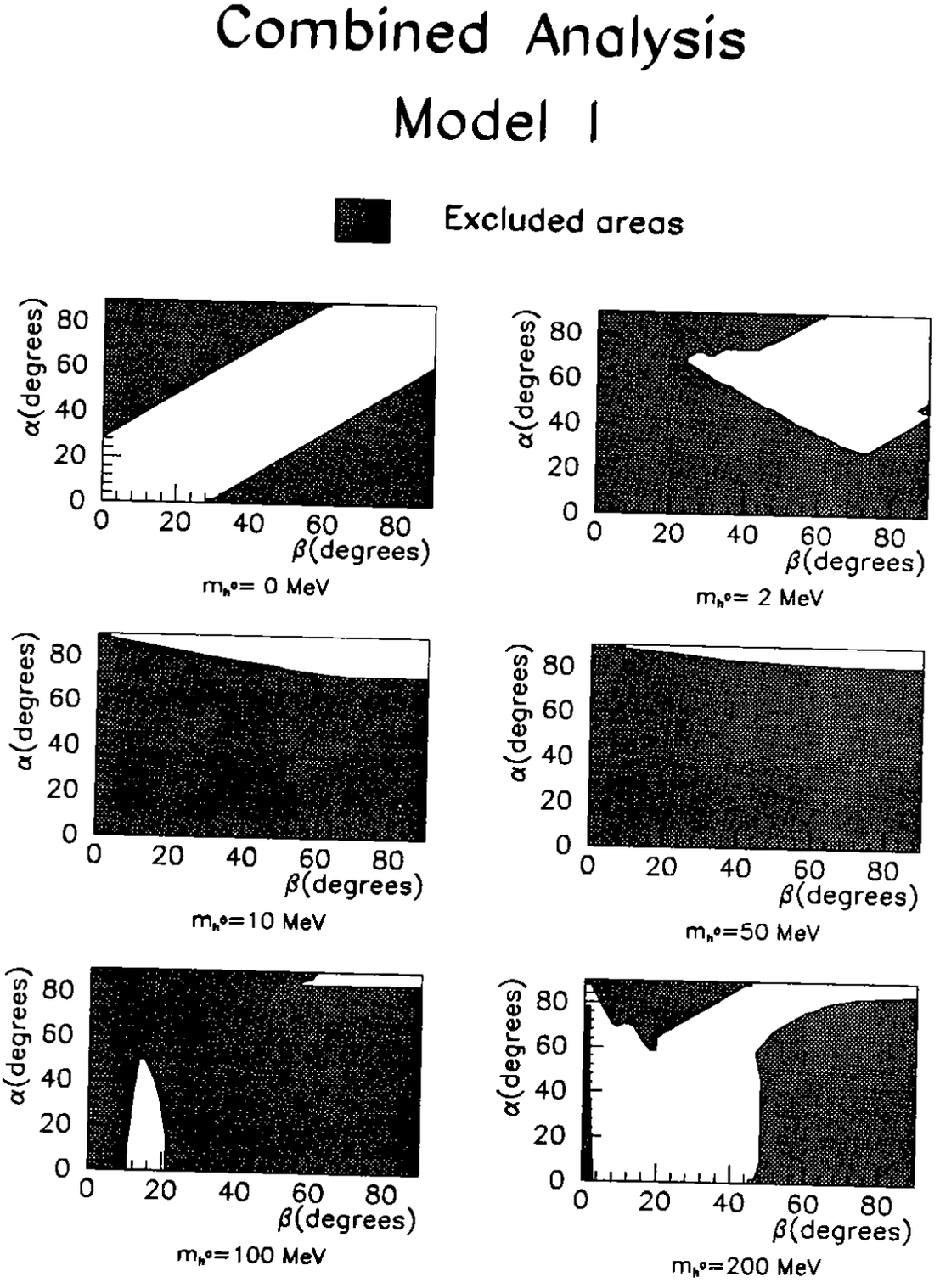

Figure 8.a: Areas in the (α, β) plane excluded at 90% C.L. by the combined analysis for different Higgs masses ($m_{h^0} = 0, 2, 10, 50, 100, 200$ MeV) in *Model I*

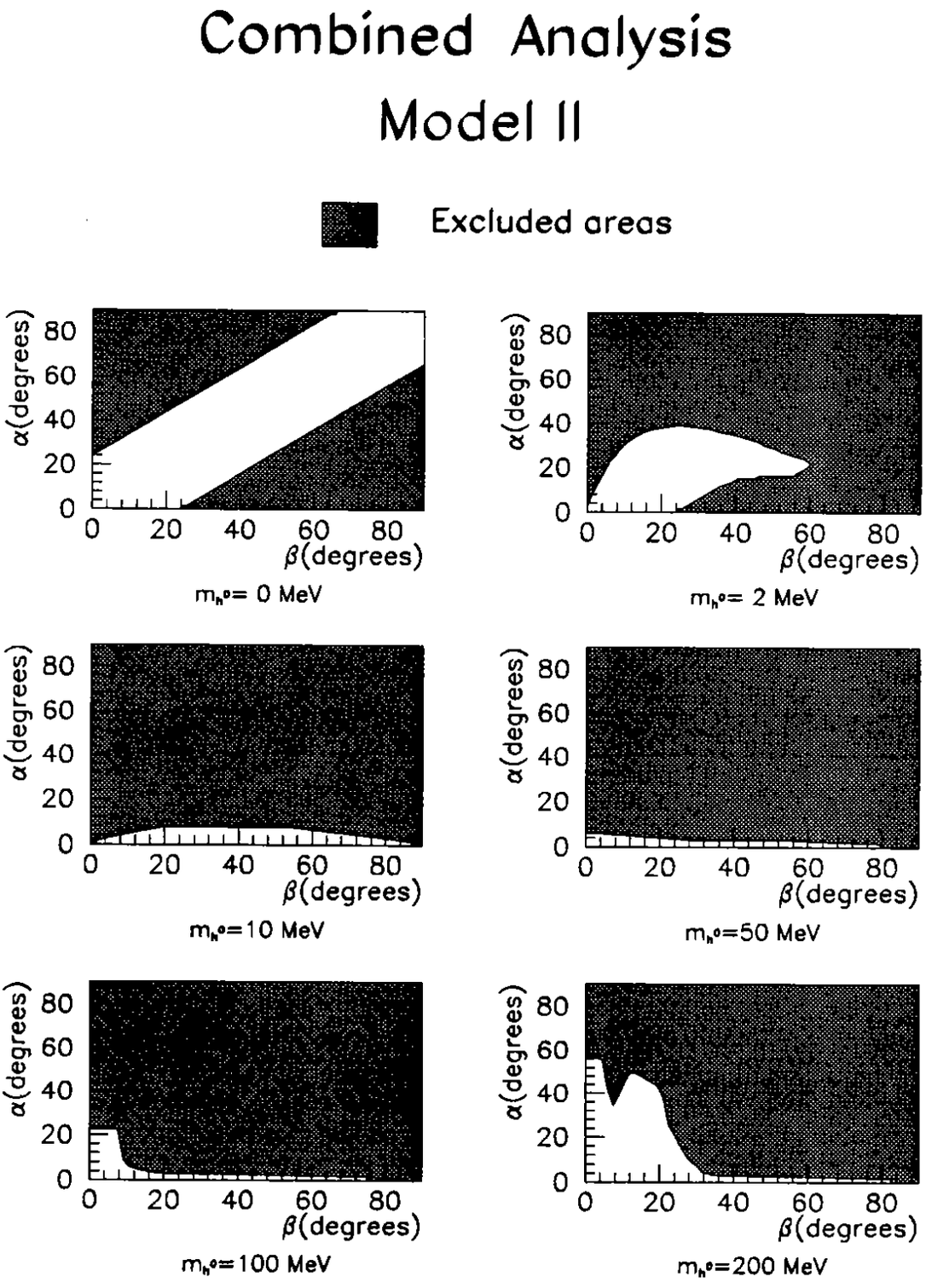

Figure 8.b: Areas in the (α, β) plane excluded at 90% C.L. by the combined analysis for different Higgs masses ($m_{h^0} = 0, 2, 10, 50, 100, 200$ MeV) in *Model II*

Imprimé au CERN. Prix: 0.55 Fr.